

## New force-field parameters for molecular simulations of *s*-triazine and cyanurate-containing systems. 2—Application and comparison with different simulation methods

R.D. Allington<sup>a,\*</sup>, D. Attwood<sup>b</sup>, I. Hamerton<sup>a</sup>, J.N. Hay<sup>a</sup>, B.J. Howlin<sup>a</sup>

<sup>a</sup>*Department of Chemistry, School of Physics and Chemistry, University of Surrey, Guildford, Surrey, GU2 7XH, UK*

<sup>b</sup>*British Aerospace (Operations) Ltd, Sowerby Research Centre, Filton, Bristol, BS12 7QW, UK*

### Abstract

The efficiency of new force-field parameters for triazines derived from analysis of crystal data of cyanurates (described previously) is demonstrated. A comparison of the molecular mechanics results with semi-empirical and ab initio methods is presented and the molecular mechanics approach is shown to give acceptable results for a fraction of the computational effort of the molecular orbital methods.

© 2002 Elsevier Science Ltd. All rights reserved.

**Keywords:** Force-field parameters; Molecular simulations; Cyanate esters

### 1. Introduction

Cyanate esters (CEs) are now becoming established as a promising family of high performance polymers, having been first developed commercially in 1967 and initially employed in the burgeoning microelectronics market in the 1970s. The cure proceeds through the formation of cyanurate rings (*s*-triazine rings linked by aryl ether linkages) and the cured resin develops interesting physical and mechanical properties. For instance, glass transition temperatures ( $T_g$ s) of untoughened, neat resins fall in the range 190–290 °C, but this is accompanied by good fracture toughness ( $G_{Ic} = 140$ –210 J/m<sup>2</sup>), low moisture absorption and low dielectric loss characteristics [1].

The application of CEs to aerospace materials (as advanced composite matrices) is a more recent development and this places them in direct competition for the market share of epoxy and bismaleimide (BMI) resins. However, being at an earlier stage of development than both of these more established products, they are currently somewhat more expensive, and recent commercial developments have involved the preparation of binary (CE/BMI) blends [2] or ternary (CE/BMI/epoxy) blends [3]. In order for CEs to develop the neat resin properties in advanced composites, several strategies are commonly adopted. The toughness of

the composite may be enhanced by the formulation of a toughening agent, such as an engineering thermoplastic (e.g. poly(arylene ether sulphone)) while the treatment of the fibres (through electrolytic oxidation) and sizing is vital to optimise the compatibility between resin and fibre. This is of particular importance in the case of CEs because the curing resin does not develop strongly polar groups (the cyanurate rings contain alternate carbon and nitrogen or oxygen atoms—hence the dipoles are balanced) to assist with matrix/fibre adhesion [4]. This study examines the importance of this aspect through the application of inverse gas chromatography and builds on a successful study of the nature of the polyacrylonitrile (PAN) fibre surface using molecular simulation techniques [5].

Molecular modelling is fast becoming established as a viable method for calculating mechanical and physical properties of polymers. As the speed and reliability of the methods improve, they will offer the potential for quick pre-screening of materials for desirable properties before embarking on a potentially laborious synthesis, involving much staff time and the potential for the generation of chemical waste. It is possible with current methods to calculate elastic moduli from very simple molecular models to the correct order of magnitude, e.g. the experimental value of Young's modulus for a linear epoxy is  $3.8 \pm 0.3$  GPa and that from simulation is  $5.8 \pm 2.4$  GPa. The experimental  $T_g$  for the same system is 358 K and that from simulation 380 K [6]. We have also used molecular

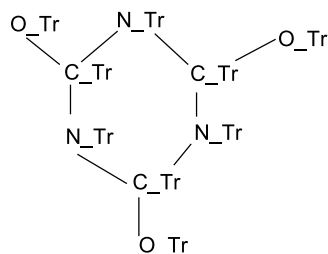
\* Corresponding author. Address: Defence Science and Technology Laboratory, Farnborough, Hampshire, GU14 0LX, UK.

E-mail address: b.howlin@surrey.ac.uk (B.J. Howlin).

Table 1

New force-field parameters to be used with the DREIDING2.21 force-field

## (a) Atom type naming in the triazine ring



New atom types	Dreiding equivalents
C_Tr	C-R
N_Tr	N-R
O_Tr	O-R

## (b) Bond parameters

Atom type 1	Atom type 2	Potential type	Force constant (kcal/mol Å <sup>2</sup> )	'Ideal' bond length (Å)
C_Tr	H	Harmonic	700.0000	1.0200
N_Tr	C_Tr	Harmonic	1499.0000	1.3220
O_Tr	C-33	Harmonic	700.0000	1.4200
O_Tr	C-R	Harmonic	1050.0000	1.3500
O_Tr	C_Tr	Harmonic	1499.0000	1.3390

## (c) Angle parameters

Atom type 1	Atom type 2	Atom type 3	Potential type	Force constant (kcal/mol Å <sup>2</sup> )	Ideal angle (°)
O_Tr	C-R	C-R1	Theta-harm	100.0000	120.0000
O_Tr	C-R	C-R	Theta-harm	100.0000	120.0000
N_Tr	C_Tr	H-	Theta-harm	100.0000	120.0000
N_Tr	C_Tr	N_Tr	Theta-harm	185.4000	127.7240
O_Tr	C_Tr	N_Tr	Theta-harm	100.0000	120.0000
C_Tr	N_Tr	C_Tr	Theta-harm	185.4000	112.2520
C_Tr	O_Tr	C-33	Theta-harm	100.0000	109.4712
C_Tr	O_Tr	C-R	Theta-harm	100.0000	120.0000

## (d) Improper torsion parameters

Atom type 1	Atom type 1	Atom type 1	Atom type 1	Potential type	Force constant (kcal/mol Å <sup>2</sup> )	$\omega_0$
C_Tr	X	X	X	Umbrella	280.2150	0.0000
O_Tr	X	X	X	Umbrella	280.2150	0.0000

simulation to predict the  $T_g$  of a system where the experimental  $T_g$  is unknown, i.e. the predicted  $T_g$  from molecular dynamics simulation of 1-(*N*-pyrrolo)-6-(4-cyano-4'-biphenyloxy)hexane is between 390 and 400 K [7].

In a previous paper [8] we have determined improved values of bond lengths and angles to describe the *s*-triazine and cyanurate moieties by analysis of X-ray crystallographic data and semi-empirical quantum mechanics (QM) calculations. In this work we compare molecular simulations of a series of molecules containing the *sym*-triazine unit using conventional and improved parameters and also draw some fundamental conclusions about the electronic and structural properties of this heteronuclear aromatic unit.

## 2. New force-field parameters for cyanurate systems

The previous paper in this series [8] presented the analysis of x-ray data of cyanurate containing compounds and derived a new set of parameters for simulating these systems using the DREIDING2.21 force-field [9]. The parameters derived from this analysis are given in Table 1. The first part of the table gives the new atom type names for the atoms in the cyanurate ring, the second part gives the Dreiding equivalents and the new bond, angle and umbrella inversion parameters follow for bonds, angles and inversions involving these atom types. The full force-field file is available from the authors on request.

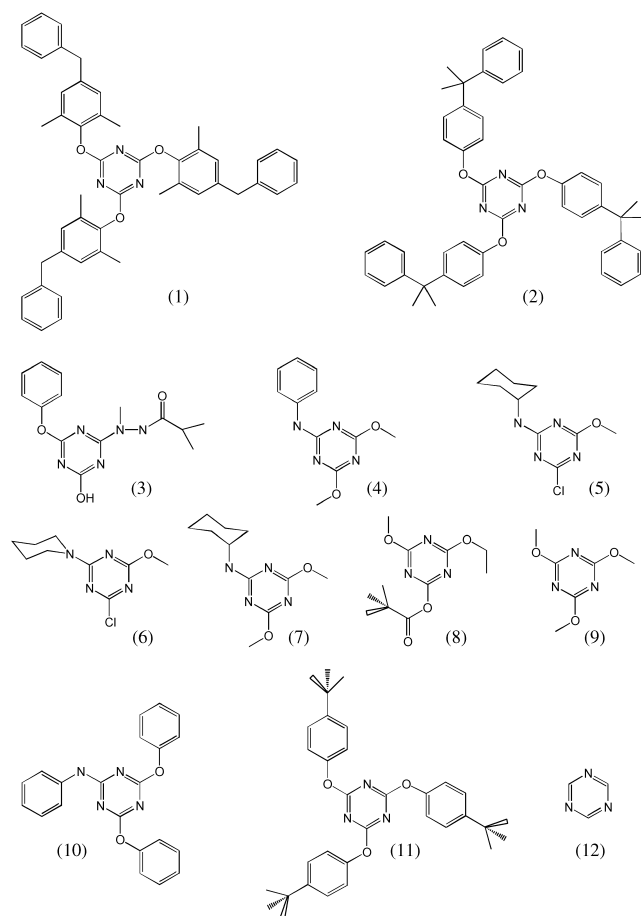


Fig. 1. Structures of molecules studied in this work (crystal data obtained from Refs. [15–24]).

Table 2

Mean bond lengths and internal bond angles of the *sym*-triazine ring unit for crystal structures, optimised using the DREIDING2.21 force-field and QEq charge calculation

	$r_{\text{C-N}} (\text{\AA})$		$\theta_{\text{N-C-N}} (^{\circ})$		$\theta_{\text{C-N-C}} (^{\circ})$	
	$\mu$	$\sigma$ (%)	$\mu$	$\sigma$ (%)	$\mu$	$\sigma$ (%)
1	1.347	0.266	120.7	0.300	119.3	0.367
2	1.346	0.432	120.3	0.504	119.7	0.715
3	1.350	0.296	119.2	1.424	120.8	1.513
4	1.352	0.389	119.7	0.782	120.3	0.760
5	1.352	0.562	119.4	0.272	120.6	0.711
6	1.349	0.655	119.5	1.312	120.4	1.072
7	1.347	0.292	120.4	0.369	119.6	0.435
8	1.348	0.706	120.7	0.301	119.3	0.330
9	1.348	0.467	120.2	0.794	119.8	0.695
10	1.349	0.564	119.2	0.812	120.7	0.791
11	1.349	0.223	119.7	0.757	120.3	0.801
Average	1.349	0.425	119.9	0.705	120.1	0.760

Table 3

Mean bond lengths and internal bond angles of *sym*-triazine ring for crystal structures containing the cyanurate unit, optimised using the RDA-DR2.21-Inv force-field and QEq charge calculation

	$r_{\text{C-N}} (\text{\AA})$		$\theta_{\text{N-C-N}} (^{\circ})$		$\theta_{\text{C-N-C}} (^{\circ})$	
	$\mu$	$\sigma$ (%)	$\mu$	$\sigma$ (%)	$\mu$	$\sigma$ (%)
1	1.335	0.239	125.8	0.600	111.8	0.787
2	1.335	0.191	125.9	0.450	112.1	0.525
9	1.336	0.336	125.6	0.567	112.3	0.613
11	1.336	0.226	125.7	0.615	112.8	0.312
Average	1.335	0.248	125.7	0.609	112.4	0.470

### 3. Comparison of force-fields by molecular mechanics

#### 3.1. Molecular mechanics optimisations of crystal structures

The adapted force-field terms have been compared with the standard values of the DREIDING2.21 force-field [9] to assess how both sets of parameters affect the optimisation process. From the crystal structure co-ordinates (Fig. 1), geometry optimisation was performed, using the conjugate gradients [10] routine until a difference of less than 0.04 kJ/mol was achieved between successive steps. The appropriate force-field terms were used in conjunction with the QEq charge calculation [11]. Although the experimental crystal structures represent the observed conformation of the molecules and their packing, it is interesting to see how this changes when computational methods are employed. Structures were optimised, without the unit cell packing constraints, using Cerius<sup>2</sup> v.2.0 on a Silicon Graphics Indy workstation.

The data in Tables 2 and 3 show how the X-ray crystal structure coordinates are changed under the influence of different force-field parameters. Dealing firstly with the DREIDING2.21 optimised data, in terms of the *sym*-triazine unit the mean C–N bond length is overestimated in every case, indeed the bonds lengthen from the crystal coordinates to a mean value greater than the equilibrium ( $r_0$ ) value of 1.34 Å [12]. The mean bond angles for the 12 structures deviate by as much as 0.8° from the equilibrium value of 120°, yet averaged over all of the crystal units the differences are only 0.1° from the equilibrium value. An inspection of the DREIDING2.21 parameters describing the cyanurate system shows that these are exactly the same as those used to describe a benzenoid *sym*-triphenoxy functionality [9].

Standard deviations in the bond lengths are lower in the DREIDING2.21 optimised data than the crystal data for all molecules. In the N–C–N bond angle measurements, standard deviations are higher for the DREIDING2.21 optimised cyanurates (molecules 1,2,9 and 11) yet lower than those in the crystal data [8] for all other molecules. There is no such trend in the C–N–C bond angles with

Table 4

Mean bond lengths and internal bond angles of *sym*-triazine ring for crystal structures, optimised from disordered atom positions using the DREIDING2.21 force-field and QEq charge calculation

	$r_{\text{C-N}} (\text{\AA})$		$\theta_{\text{N-C-N}} (^{\circ})$		$\theta_{\text{C-N-C}} (^{\circ})$	
	$\mu$	$\sigma$ (%)	$\mu$	$\sigma$ (%)	$\mu$	$\sigma$ (%)
1	1.348	0.282	120.6	0.251	119.4	0.381
2	1.346	0.431	120.3	0.491	119.7	0.714
3	1.350	0.550	118.8	1.973	121.2	2.222
4	1.352	0.390	119.7	0.782	120.3	0.758
5	1.352	0.563	119.4	0.273	120.6	0.713
6	1.349	0.517	120.4	0.626	119.6	0.429
7	1.350	0.349	120.3	0.386	119.7	0.396
8	1.347	0.670	121.0	0.660	118.9	0.396
9	1.352	0.592	118.7	0.626	121.2	0.465
10	1.349	0.532	119.1	0.792	120.8	0.801
11	1.349	0.222	119.7	0.756	120.3	0.800
Average	1.349	0.445	119.8	0.703	120.2	0.751

roughly one-half of the simulated angle standard deviations being higher than experiment.

For comparison with the DREIDING2.21 optimisations, only the four cyanurate species, molecules 1, 2, 9 and 11 (both conformations), have been considered. New force-field parameters have not been set for all possible R groups (e.g. no specific terms for bonding between ring carbon atoms and substituents such as chlorine have been added) as the end application of the force-field is for polycyanurate systems and in particular commercial polymers (which generally bear aryl and bisphenyl moieties).

The optimisations using the new force-field parameters show an improvement over the DREIDING2.21 calculations in all aspects of the *sym*-triazine ring structure as expected. The mean C–N bond lengths of 1.335–1.336 Å are closer to the crystal data [8] than the DREIDING2.21 values, lying roughly equidistant from both sets of data. Other energy terms, particularly non-bonded electrostatic and dispersion (Lennard–Jones 12,6) interactions are believed to inhibit the C–N bond lengths being closer to their  $r_0$  value of 1.322 Å [12]. The standard deviations in the bond lengths are lower for molecules 1, 2 and 9 and comparable with 11 optimised

Table 5

Mean bond lengths and internal bond angles of *sym*-triazine ring for crystal structures containing the cyanurate unit, optimised from disordered atom positions using the new force-field parameters and QEq charge calculation

	$r_{\text{C-N}} (\text{\AA})$		$\theta_{\text{N-C-N}} (^{\circ})$		$\theta_{\text{C-N-C}} (^{\circ})$	
	$\mu$	$\sigma$ (%)	$\mu$	$\sigma$ (%)	$\mu$	$\sigma$ (%)
1	1.333	0.253	125.8	0.690	111.6	0.935
2	1.335	0.191	125.9	0.450	112.1	0.532
9	1.336	0.354	125.7	0.556	112.4	0.727
11	1.335	0.186	125.7	0.518	112.5	0.463
Average	1.335	0.247	125.7	0.607	112.3	0.555

using DREIDING2.21. This is a result of the larger force constant assigned to the new bond stretching term.

The internal ring bond angles at both carbon and nitrogen are clearly much closer to the crystal structures than using DREIDING2.21. Whereas the calculated angles at C–N–C fall within experimental error, the N–C–N angles are a slight underestimate of those found experimentally. This is due to the coupling of this term with the umbrella inversion also centred on this carbon atom. Standard deviations are lower than those for the corresponding DREIDING2.21 parameter for structures 2, 9 and 11, yet greater than found in the crystal structure data. This can be attributed to the removal of the symmetry constraints in treating each molecule in the crystal cell individually (?).

### 3.2. Molecular mechanics optimisations of disordered crystal coordinates

To probe further the efficiency of geometry optimisation using both adapted and original force-field terms, an analogous series of optimisations was performed using the same criteria as before, but introducing positional disorder to all of the atoms in the crystal cell. The atomic positions were ‘disordered’ simultaneously by 0.1 Å in a random direction (assigned as part of a computational routine). This procedure was performed five times. The subsequently optimised models have been analysed in terms of their *sym*-triazine bond lengths and internal bond angles in a similar fashion to that presented previously.

Even after the molecular conformations have been considerably perturbed, the optimisation routine returns the *sym*-triazine unit to a geometry very similar to that produced when starting from the crystal coordinates. For the DREIDING2.21 optimised structures (Table 4) both the mean C–N bond lengths and their standard deviations are comparable with those given in Table 3. For the N–C–N bond angle, although the range of mean values for the DREIDING2.21-optimised disordered data is greater than that for the non-disordered optimisations (118.8–121.0° vs. 119.2–120.7°), the averages of these two sets of data differ by only 0.1°. The same applies to the C–N–C bond angle data in Tables 2 and 3. The standard deviation ( $\sigma$ ) of the ring angle data ( $\theta$ ) for the optimised disordered structures is comparable with that of the optimised crystal structures [8], indicating a good efficiency of the optimisation routine when applied to these disordered coordinates (albeit with inaccurate bond length and angle parameters).

Using the new force-field parameters in optimising the disordered cyanurate crystal structures (Table 5), the mean C–N bond lengths and standard deviations are comparable with those listed in Table 3. The bond angle data ( $\theta$ ) for both C–N–C and N–C–N also show the effectiveness of the optimisation routine on the disordered coordinates.

Table 6

Mean bond lengths and internal bond angles of the *sym*-triazine ring moiety for single molecules used in the set of crystal structures, optimised from DREIDING2.21-refined atom positions using the PM3 Hamiltonian

	$r_{\text{C-N}} (\text{\AA})$		$\theta_{\text{N-C-N}} (^{\circ})$		$\theta_{\text{C-N-C}} (^{\circ})$	
	$\mu$	$\sigma$ (%)	$\mu$	$\sigma$ (%)	$\mu$	$\sigma$ (%)
1	1.369	0.590	123.0	1.260	117.0	1.648
2	1.370	0.368	124.0	0.727	116.0	0.979
3	1.372	0.489	124.3	1.155	115.6	0.949
4	1.374	0.601	124.6	1.115	115.4	0.656
5	1.370	0.629	123.6	0.890	116.4	0.749
6	1.370	0.763	123.6	1.052	116.4	0.798
7	1.372	0.504	124.4	1.328	115.6	0.949
8	1.370	0.391	125.0	0.167	115.0	0.050
9	1.371	0.000	125.1	0.000	114.9	0.000
10	1.373	0.604	124.3	1.138	115.7	0.672
11	1.370	0.080	125.1	0.000	114.9	0.000
12	1.358	0.000	126.1	0.000	118.4	0.000
Average	1.370	0.419	124.4	0.734	115.9	0.622

#### 4. Conclusions regarding molecular structure optimisations

New parameters to describe the conformation of *sym*-triazine units have been generated from analysis of X-ray crystal structures [8] and applied to computational molecular mechanics force-field calculations on systems containing this moiety. They are found to be an improvement over existing force-field data when used in optimisations of these structures. The efficiency of the optimisation of randomly disordered structures has also been analysed and is found to produce acceptable results for all the cases studied.

With respect to the crystal data upon which they are based [8], the new force-field values do tend to overestimate the C–N bond lengths, probably arising from the conflict between the short bond length and the repulsive force of two atomic centres approaching each other (represented by a Lennard–Jones 12,6 potential). The internal ring angle at carbon is also underestimated by ca. 2°, being offset by an umbrella inversion term about this carbon atom with a relatively large force constant trying to maintain a planar geometry (analogous to  $sp^2$  hybridisation of the carbon atom).

##### 4.1. Quantum mechanical structure optimisations

The molecules from the crystal data series were initially geometry optimised using the DREIDING2.21 force-field and QEq charge assignment by the conjugate gradients method until the energy between successive steps fell below 0.04 kJ/mol. In this way the improvement of the quantum mechanical methods on the original DREIDING2.21 parameters could be analysed. The data files for the quantum mechanical structure optimisations were generated from these structures, with the inclusion of explicit hydrogen atoms.

The DREIDING2.21-refined structures were further optimised using the PM3 Hamiltonian within the MOPAC semi-empirical package. The optimised bond lengths and bond angles for the *sym*-triazine units are given in Table 6.

Using this semi-empirical quantum mechanical method the C–N bond lengths are overestimated by ca. 3% compared with the crystal structure data, indeed they lie even further from the crystal data than the DREIDING2.21-optimised values. The standard deviations in the C–N bond lengths are lower than in the crystal data for all molecules except number 1. It must be noted, however, that these calculations have been performed on single molecules in vacuo, whereas the molecular mechanics force-field calculations were derived from units of the crystal cells, thereby implicitly including intermolecular interactions in the parameters.

The mean C–N value of 1.370 Å lies above both the C–N double and aromatic resonance bond lengths of 1.331 and 1.338 Å, respectively, although below the standard C–N single bond length of 1.468 Å [12]. This implies that the PM3 method recognises that these bonds have more double bond character than a single  $\sigma$  bond. The shortest calculated mean C–N bond length is found for the *sym*-triazine molecule (number 12). Thus, the computational treatment of substituents bonded to the ring carbon atoms results in a withdrawal of electron density from the aromatic triazine  $\pi$ -system, resulting in a longer mean C–N bond length for these molecules (numbers 1–11).

The N–C–N and C–N–C internal ring bond angles ( $\theta$ ) deviate from the hexagonal 120° values in the correct directions, i.e. the angle at carbon increases and that at nitrogen decreases, but not to the extent of the experimental measurements. This is an improvement over the DREIDING2.21 molecular mechanics calculations; however, it is not as accurate as the optimisations with the new force-field parameters.

The standard deviations in the internal bond angles ( $\theta$ ) are generally lower than those observed in the crystal data, the exceptions being molecules 1 and 2 for N–C–N and 1, 2 and 10 for C–N–C. Molecules 9 and 12 are computed as having a three-fold symmetry axis, thus their standard deviations are zero for the ring bond and angle data. Although molecules 1 and 2 also have the potential to exhibit three-fold symmetry, this was not calculated using this method. This anomaly may be due to the greater number of atoms involved, resulting in a significant increase in the number of degrees of freedom and therefore a more complex potential energy surface.

Structures 3–12 were also optimised using the 6-31G\* basis set in the GAUSSIAN94 package [13]. Owing to the number of atoms involved, and hence the necessity for a long period of calculation time, molecules 1 and 2 were optimised using the 3-21G basis set (Table 7).

The optimisations of the 12 molecules using ab initio methods show an improvement over the semi-empirical QM calculations in terms of structural ring parameters. C–N



Table 7

Mean bond lengths and internal bond angles of the *sym*-triazine ring moiety for single molecules used in the set of crystal structures, optimised from DREIDING2.21-refined atom positions using the 3-21G or 6-31G\* basis sets through the GAUSSIAN computational chemistry program

	$r_{C-N}(\text{\AA})$		$\theta_{N-C-N} (^{\circ})$		$\theta_{C-N-C} (^{\circ})$	
	$\mu$	$\sigma$ (%)	$\mu$	$\sigma$ (%)	$\mu$	$\sigma$ (%)
1	1.323	0.225	124.2	0.007	115.8	0.006
2	1.325	0.794	123.8	0.006	116.2	0.012
3	1.318	0.759	126.2	0.910	113.8	0.444
4	1.321	0.920	125.9	0.632	114.1	0.297
5	1.320	1.108	126.3	1.416	113.7	0.759
6	1.327	1.852	124.3	2.359	115.7	1.292
7	1.322	0.752	125.8	1.139	114.2	0.603
8	1.316	0.750	126.8	0.752	113.7	0.401
9	1.319	0.710	126.1	0.001	113.9	0.002
10	1.319	0.944	126.1	0.889	113.9	0.446
11	1.316	0.499	126.4	0.019	113.6	0.005
12	1.318	0.002	125.6	0.000	114.4	0.000
Average	1.320	0.777	125.6	0.678	114.4	0.356

bond lengths are comparable with those of the original crystal data [8], although in general the mean bond length is slightly underestimated. Standard deviations in the calculated bond length data are lower than experiment except for molecules 4, 6, 11 and 12, although the difference in the standard deviations of molecule 12 is negligible.

The mean internal ring bond angles at carbon are generally closer to the experimentally observed values than those of the semi-empirical calculations, the exceptions being molecules 2 and 12. All N–C–N angles still lie ca. 2° below the crystal data values, however, with standard deviations less than found in the crystal data [8]. The mean bond angles at C–N–C conversely are all wider than found experimentally, by as much as 3.6° in the case of molecule 1. The overall mean value of 114.4° lies 1.8° above that of the crystal data. Standard deviations ( $\sigma$ ) in the calculated C–N–C bond angles are lower in all cases than the corresponding experimental values, although this phenomenon may arise from a lack of intermolecular interactions.

The close proximity of the C–N bond lengths to the observed values indicates that these are calculated more accurately using a full electron treatment than the semi-empirical valence electron calculations. It is possible that the ‘closed shell’ radius used in the PM3 Hamiltonian is too large, thus the ring atom centres do not approach each other due to repulsive interactions. In a full quantum mechanical treatment the inclusion of all electrons explicitly, and polarisation functions in particular to permit off-centre bonding, allows for perturbation to counter this effect and thus leads to a shorter C–N bond length than the semi-empirical calculations. As also observed in the crystal data, the mean ab initio calculated bond length is less than for a standard carbon–carbon aromatic or double bond, showing the bond order of the C–N bonds to be greater than the aromatic bonds in benzene. The values are also lower than

the carbon–nitrogen aromatic or double bonds observed in pyridine and pyrazole, respectively.

#### 4.2. Comparison of molecular and quantum mechanical structure optimisations

The different methods of energy calculation, and structure optimisation resulting from this, reveal how the various treatments interpret and deal with the aromatic nature of the *sym*-triazine unit by analysis of the molecular conformation. The simple molecular mechanics ‘ball and spring’ approach can be refined by altering parameters in the force-field, as has been shown in this work.

When electrons are considered, as in the semi-empirical and ab initio quantum mechanical methods, conclusions can be drawn as to their distribution and resulting molecular physical properties. In terms of aromaticity, the *sym*-triazine moiety conforms to the standard rules: it has a relatively planar conformation, contains  $2n + 2$   $\pi$  electrons; a p orbital on every atom on the ring; and a structure of conjugated double bonds. The conformation of the ring is not absolutely planar, exhibiting a small torsion angle of ca. 1° experimentally. This may be due to the short C–N bond length observed and the bond angle behaviour about the carbon atoms in the ring.

The effect of ring substituents on both the aromatic nature and bond lengths of the ring can be explained by considering quantum mechanically calculated electron densities at specific atomic positions in the set of molecules. In *sym*-triazine (molecule 12) the partial charges on the carbon atoms are calculated as 0.0134 (PM3) and 0.2775 (6-31G\*), whereas those on the nitrogen atoms are –0.1572 (PM3) and –0.5079 (6-31G\*). The sum of all six (carbon and nitrogen) atoms is therefore –0.4318 (PM3) and –0.6913 (6-31G\*). This means that the six-membered ring is relatively electron rich, resulting in stronger and shorter bonds between the carbon and nitrogen atoms. This is observed experimentally in the mean C–N bond length being less than that for C–N aromatic or even C=N double bonds.

Considering the trimethoxy-*sym*-triazine structure (molecule 9), this has three O–CH<sub>3</sub> groups evenly substituted on alternate carbon atoms around the triazine ring. In conventional aromatic chemistry the methoxy unit is one of the strongest electron donating activators (behind NH<sub>2</sub> and OH), directing electrophilic substitution, and corresponding electron density, to the *ortho* and *para* positions [14]. The activation arises from an electron donating resonance effect that more than compensates for the electron withdrawing inductive effect.

This theory suggests an increase in ring electron density, particularly on the nitrogen atoms, being in the *ortho* and *para* positions relative to the methoxy groups. The greater negative charge is computed in the quantum mechanical calculations, with the partial electronic charge at nitrogen increasing from –0.1572 to –0.2752 for PM3 and from

–0.5079 to –0.6838 for 6-31G\* calculations. The overall electron density of the ring system, however, is depleted for trimethoxy-*sym*-triazine. The partial electron charge decreases to –0.1596 for the PM3 calculations and even becomes positive at 0.6782 for the 6-31G\* calculations. This 6-31G\* value suggests that, contrary to the theoretical electron donating activation of aromatic ring systems, the electron withdrawing inductive nature of this substituent outweighs the electron donating resonance effect.

Nevertheless, the ring electron density decreases upon addition of any of the substituents (other than hydrogen) to the ring, as studied in this work; they act as electron withdrawing groups. This is reflected in the increase in mean C–N bond lengths observed in the crystal structure analyses and 6-31G\* (for all except molecule 11) and PM3 structure optimisations.

This suggests that, owing to the heteroatomic yet aromatic character of the *sym*-triazine moiety, its electronic structure is more prone to influence by substituents than the monoatomic analogue benzene.

## 5. Conclusions

The newly defined force-field terms change the characteristics of the *sym*-triazine and cyanurate units markedly. In particular, the force constants for stretching, bending and inversion motions about the ring are much greater than those used in the DREIDING2.21 force-field. The flexibility of a polycyanurate network would therefore have to rely much more on the backbone structure and ether oxygen linkages as their force constants are smaller in comparison.

The optimisations on cyanurate systems using the new force-field parameters produce structures closer to those found in the crystal data than semi-empirical calculations and a better representation of internal ring bond angle data than *ab initio* quantum mechanical calculations for a fraction of the computational effort involved in the calculation. These quantum mechanical calculations have not only been used for comparison with the new force-field terms, but to explain some phenomena observed in the crystal structures, particularly substitution effects and C–N bond lengths.

The use of a rapid, computationally inexpensive molecular mechanics routine, incorporating modified force-field parameters, to calculate conformational beha-

viour in these systems has been shown to generate structures closer to experimental crystal data than lengthy semi-empirical or full *ab initio* quantum mechanical computational techniques. With the ever-increasing exploitation of polymers containing these chemical moieties in high technology structural and functional applications, the calculation of bulk properties based on these types of chemical modelling methods will continue to grow in importance.

## References

- [1] Hamerton I, editor. Chemistry and technology of cyanate ester resins. Glasgow: Blackie; 1994. and references cited therein.
- [2] Nair CPR, Francis T, Vijayan TM, Krishnan KJ. J Appl Polym Sci 1999;74:2737.
- [3] Gotro JT, Appelt BK, Papathomas KI. Polym Compos 1997;8:39.
- [4] Mackenzie PD, Malhotra V. Chemistry and technology of cyanate ester resins. In: Hamerton I, editor. Properties of reinforced cyanate ester resins. ; 1994. p. 258–81. Chapter 9, and references cited therein.
- [5] Allington RD, Attwood D, Hamerton I, Hay JN, Howlin BJ. Composites Part A 1998;29:1283.
- [6] Barton JM, Deazle AS, Hamerton I, Howlin BJ, Jones JR. Polymer 1997;38:4305.
- [7] Rabias I, Hamerton I, Howlin BJ, Foot PJS. Comput Theor Polym Sci 1998;8:265.
- [8] Allington RD, Attwood D, Hamerton I, Hay JN, Howlin BJ. Comput Theor Polym Sci 2001;10:467.
- [9] Mayo SL, Olafson BD, Goddard III WA. J Phys Chem 1990;94:8897.
- [10] Leach AR. Molecular modelling: principles and applications. Harlow: Longman; 1996.
- [11] Rappé AK, Goddard III WA. J Phys Chem 1991;95:3358.
- [12] Lide DR, editors. Handbook of chemistry and physics (section 9). Florida: CRC Press, 1992–3.
- [13] GAUSSIAN94 by Frisch A, Frisch MJ, Foresman JB, 1994. Marketed by Gaussian Inc., Pittsburgh.
- [14] McMurry J. Organic chemistry. California: Brooks/Cole; 1992. p. 573.
- [15] Allington RD, Brownhill A, Garbarczyk J, Hamerton I, Howlin BJ, Lagocki G. Unpublished work.
- [16] Reck C, Bannier G, Just M, Goldhahn F. Crystallogr Res Tech 1985; 20:1341.
- [17] Glówka ML, Iwanicka I. Acta Crystallogr 1991;C47:1036.
- [18] Glówka ML, Iwanicka I. Acta Crystallogr 1991;C47:616.
- [19] Glówka ML, Iwanicka I. Acta Crystallogr 1989;C45:1762.
- [20] Glówka ML, Iwanicka I. Acta Crystallogr 1990;C46:2211.
- [21] Glówka ML, Iwanicka I. Acta Crystallogr 1989;C45:1765.
- [22] Glówka ML, Iwanicka I. J Crystallogr Spectrosc Res 1991;21:711.
- [23] Fyfe CA, Niu J, Rettig SJ, Burlinson NE, Reidsema SM, Wang DW, Policks M. Macromolecules 1992;25:6289.
- [24] Wheatley PJ. Acta Crystallogr 1955;8:224.